Sirte University Scientific Journal(Applied Sciences) Vol.9 (2), December 2019

CFD Simulation and Optimization of 4-Digit NACA Airfoils

Abdalsalam Muftah

e-mail: salamgader@su.edu.ly

Mechanical Engineering Department, Faculty of Engineering, Sirte University

Abstract

The work presents a CFD modeling using Comsol Multiphysics to find the optimal design of wind turbine airfoils. This study has two parts, the first part is to find the optimal angle of attack of the initial NACA airfoil in different operating conditions of a wide range of Reynolds number taking into account the aerodynamics performance before and after optimization. The second part is to study the effect of decoupling camber and its position as control shape parameters on the aerodynamics performance as objectives function with varying thickness of airfoils.

The results illustrated that, compared to an initial NACA 4digit airfoil, the optimized airfoils lift to drag ratio was improved over a wide range of Reynolds number and the maximum thickness of airfoil. The results showed also that the blade with the optimized airfoil has a higher efficiency.

Keywords: *Aerodynamics, NACA airfoil, Optimization, Camber, Angle of attack, Lift and drag coefficients,*

1. Introduction

Regarding increasing demand of energy in countries like Libya, it is necessary to develop renewable energies despite huge amount of fossil fuel resources. Besides this reason, the combustion of fossil fuels results a net increase of 10 billion tons of atmospheric carbon dioxide every year, which makes it necessary to work on renewables like wind [1]. Wind turbine industry has a very good development worldwide that recommends wind as a more reliable, clean and unlimited energy resource in near future [2]. Wind energy has a growing market and some recent researches have been considering other renewables wind power generation is the fastest growing industry in energy sector, by the end of 2012, the world total installed capacity of wind turbines reached 285 GW and it was expected to reached 500 GW in the year of 2017[3]. As wind turbine

airfoil has a significant effect on turbine output power and efficiency, several researches have been performed about wind turbine airfoil optimization.

The recent publications on design optimal structures for wind turbine blades were reviewed. To create optimal blade design, the best is to generate higher lift force and provide maximum torque to the generator. We need to consider the main factors such as speed and density of the wind, geometrical shape of an airfoil including camber length, blade thickness. When designing the airfoil for wind turbine, the aspects like the maximum lift to drag ratio which represents the turbine performance must be considered.

Experimental investigations are very important due to accuracy. However, those take much time and economic and whenever we want to change a parameter about our study, it is very difficult because of time , economic and the risks of repeated experiments. Fortunately, researchers can study very fast and easily by using computational fluid dynamics (CFD) programs[4,5]. These programs can give as correct results as experimental method does. In recent years, there has been an increasing interest in morphing airfoils that can operate efficiently across a wide range of Reynolds numbers. For example, a wind turbine blade operates in a different streams of air flow, and Reynolds number (Re) varies from 10^3 to 10^6. The blade efficiency would be significantly enhanced if its sectional airfoil could adapt its shape and angle of attack to the flow conditions [6]. The benefit of adopting a variable airfoil geometry has been proven in several applications, including wind turbine blades [7,8,9,10] and aircraft wings and helicopter rotors [11,12,13]. Although the research field of airfoil design by [14, 15] and multi-objective optimization by [16, 17, 18] is well established, the optimization across a wide range of Re and airfoil shapes are an open area of research.

During the airfoil optimization process, the airfoil's geometric shape must be designed before optimization. In order to ensure that the airfoil points are smoothly and continuously connected, the mathematical parameterization method of the Bezier, PARSEC parametric curves perturbation among others methods are used in many aerodynamic studies, the merits of the parameterization method have a very significant impact on the final optimization results, and therefore it is the key factor for determining the efficiency and results of the optimization. Kulfan proposed CST parameterization method to design the airfoil coordinates and that of other geometric features: such as the camber and its position [19]. The CST parameterization method has good potential for aerodynamic optimization of 2D dimensional airfoils and three dimensional (3D) wings; thus it has also been widely applied to airfoil optimization of wind turbines [20].

The main objective of this paper is to investigate how wind turbine blades can be optimized to find the airfoil that enables a maximum lift- to- drag ratio. To make the study more general, two kinds of optimization are considered: one is based on optimizing angle of attack under different

operating Reynolds numbers, the second is based on optimizing the camber of airfoil and its position with different airfoil thicknesses. The first aim of this paper is to identify and assess a computational fluid dynamics (CFD) method that can be efficiently coupled with an optimization approach and that is capable to correctly predict the stall airfoil angle of attack which are optimized in different operating conditions of Re starting from Re = 10^3 to 10^6 to maximize the aerodynamics of airfoils. The second objectives is to optimize the maximum camber and its associated position in deferent maximum thickness of airfoils starting from th= 0.08 to 0.2 to maximize lift- to- drag ratio.

2. CFD Modeling and Simulation

A segregated, implicit solver, Comsol Multiphysics, is utilized to simulate the problem. The airfoil profile is stimulated in the Design Modeler and boundary conditions, meshes are created. With the help with the commercial CFD software Comsol, two dimensional airfoil's aerodynamic performance was simulated numerically. The control equations were Navier-Stokes equations, with the Spalart–Allmaras turbulence model.

In this work, we consider the flow around a fully parameterized NACA airfoil at different Reynolds number (Re = 10^3, 10^4 , 10^5, and 10^6) and a wide range of thickness of 0.08 to 0.2 as percent of chord. let the app's optimization solver find the optimal geometry in order to maximize the lift-to-drag ratio. The solver can be used to visualize how changes to the airfoil thickness, camber, and variation of Reynolds number affect the aerodynamics.

2.1 Geometry Generation of NACA Four-Digit Airfoil

NACA airfoil is designed generally for aircraft. Then, some designed airfoils have been also used in wind turbines. NACA-four digits airfoil or five digits types (National Advisory Committee for Aeronautics) were investigated in the literature. Generally, a lot of researchers studied lift and drag performances of NACA airfoil. Habtamu and Yingxua., have computed aerodynamic performance analysis of a symmetric NACA0018 wind turbine airfoil by using numerical simulation method. Bezier curve method uses thirteen control airfoil geometry parameters, these parameters can control local changes in upper and lower surfaces of airfoil [21]. Other parameterization methods, include the PARSEC method [22], which uses eleven specific airfoil geometry parameters and the Bezier-PARSEC method [21] which combines the Bezier and PARSEC methods. In this study, for seeking of simplicity, we use the NACA 4-digits airfoil shapes as a parameterization method [23] where the airfoil shape is defined by three parameters, maximum upper camber, m (as percentage of the cord), the second parameter, the position of the maximum upper camber from the airfoil leading edge, p (as percentage of the cord), and the last parameter describes the maximum

thickness of the airfoil (t/c), as percent of the chord length. The airfoils are denoted by NACA mpxx, where xx is the thickness to the chord ratio t/c. since these parameters are widely accepted in aerodynamics airfoil designs and satisfy the conditions and the objectives of this study. The runner airfoils are shaped with NACA-2414 of airfoil of four digits.

In a XOY plane, the airfoil coordinates (x, y) are non-dimensionless with respect to the chord, with x=0 at the leading edge ($x = {}^{s}/_{c}$) where s is the domain boundary at the airfoil, $s = 0$ at leading edge of airfoil and $s = c$ at trailing edge.

The NACA four-digit airfoils have similar thickness distribution and piecewise parabolic mean camber line.

1. Consider an airfoil of chord length c along the x-axis. Then, the thickness distribution,

y_t, is given, for $0 < x < c$, as

$$y_t = \pm 5\, tc(0.2969\sqrt{x} - 0.1260x - 0.3516x^2 + 0.2843x^3 - 0.1015x^4)$$

The maximum thickness occurs at 30% of the chord from the leading edge. That is, at $x = 0.30c$, y_t is maximum and equal to $0.5tc$. t is usually referred to as the *thickness ratio* and is equal to the ratio of maximum thickness to the chord length, i. e.,

$$t = 2\frac{Max(y_t)}{c}$$

The radius of curvature at the leading edge is $r_{l.e} = 1{:}1019t^2$

2. The mean camber line, y_c, is made of two parabolas :

(i) Forward of the maximum coordinate

$$y_c = \frac{m}{P^2}(2P^2x - x^2) \quad for\ 0 \le x < p$$

(ii) After of maximum coordinate

$$y_c = \frac{m}{(1-p)^2}((1-2p) + 2Px - x^2) \quad for\ p \le x \le 1$$

pc is the chord wise position of maximum camber, and *m* is the *camber ratio*, i. e.,

$$m = 2\frac{Max(y_c)}{c}$$

3. The total coordinates (x, y) is made of two parabolas :

(i) The upper surfaces at the NACA airfoil are defined by

$$y_{upper} = y_c + y_t \cos(\theta(x))$$

$$x_{upper} = x - y_t \sin(\theta(x))$$

(ii) The lower surfaces at the NACA airfoil are defined by

$$y_{lower} = y_c - y_t \cos(\theta(x))$$

$x_{lower} = x + y_t \sin(\theta(x))$

Where

$$\theta(x) = \begin{cases} tan^{-1}(\frac{2m}{P}(P-x) & x < P \\ tan^{-1}(\frac{2m}{(1-P\ )}(P-x)^2 & x \geq P \end{cases}$$

3. The NACA four-digit airfoils are represented by NACA 2414. The last two digits represents the airfoil maximum thickness. The first digit represents the maximum mean camber. The second digit represents the position of the maximum camber. Thus NACA0014 represents a symmetric airfoil with 14% maximum thickness, i.e., t=0.14. NACA2414 is an asymmetric airfoil with a maximum mean camber of 2% located at a distance 0.4*c*

2.2 Blade Airfoil and Parameters

The physical parameters of initial airfoil before optimization are used in the simulation as follows: Air velocity is 1 m/s, atmospheric pressure is 101325 Pa, air density is 1.225 kg/m, air temperature is 293 K, kinematic viscosity is 1.82×10^{-5} m^2/s. compressible flow ($M_a < 0.3$) , Turbulence model RANS, Turbulence model type is Spalar-Allaras. The parameters of the original NACA 2414 are presented in table. 1

Table 1 Parameters of original NACA 2414

Parameters	**Values**
Chord length, C	1
Initial maximum camber, m	0.02
Initial position of the maximum camber, P	0.4
Maximum thickness, t	0.14
Wind speed, u	1
Angle of attack, α	0^o
Reynolds Number, Re	10^5,
Computational domain, n_r	2
Density Dynamics viscosity,	$1/Re$

The methods presented herein for solving the aerodynamic design problems focus on several key findings; Performance of airfoil at operating conditions of Reynolds number or in varying maximum thickness is compromised by the need to satisfy off-design constraints. More performance might be sacrificed if the designed constraints are satisfied. Appropriate selections in respect to weights, mechanical and endurance limits might be prevented. Table 2 shows the most important objectives and constraints for airfoil optimization

.

Table. 2 Optimization Objectives and Constraints

Parameter variation	Case1 (Reynolds number=10^3, 10^4, 10^5, 10^6) Case 2(Max. thickness=0.08, 0.12, 0.16, 0.20)
Geometric constraint	Max. camber (m) must be less than 10% of chord length Position of camber (p) $0.3 \leq p \leq 0.7$
Angle of attack (α) constraint	$-15^o \leq \alpha \leq 15^o$
Aerodynamic constraint	Lift to drag ratio not less than original one
Objective	Maximize lift to drag ratio
Termination condition	No change in lift to drag ratio for 1000 iterations

2.3 Airfoil Grid Meshing

In the present work, the simulation of the blade airfoil begins with the airfoil calculating field firstly. The appropriate selection of the calculation of the flow area has an important influence on the simulation results. In principle, the boundary is as far as possible [25], but it also increases the amount of computation and the result may not be the best. According to the experiences of predecessors [26] the selected airfoil grid shape is free C-shape which can make the mesh generation convenient. The free (unstructured) meshing method is used to mesh the airfoil grid, the unstructured meshing method has been also used by [27, 28]. The mesh is calibrated for fluid dynamics models. In this study, two size of meshes are used to mesh the entire domain and boundaries of airfoil for turbulent and laminar flow as defined in Table 3, Low Reynolds number simulations are varied from fine up to extra fine grids with the Laminar Flow interface in the CFD Module, the maximum element size was set at 0.14 and the minimum was 0.004 producing 12072 elements, while at the boundary surface, the maximum element size was set at 0.052 and the minimum was 0.0004 producing 234 boundary elements. The high Reynolds number simulations are performed on a fine mesh to finer with the Turbulent Flow interface in the CFD Module, the maximum element size was set at 0.14 and the minimum was 0.004 producing 7566 elements, while at the boundary surface, the maximum element size was set at 0.112 and the minimum was 0.0016 producing 204 boundary elements. The resolution and density of the mesh is more condensed in regions where superior computational accuracy is needed, such as the near wall region of the airfoil. In high quality unstructured grid is shown in Fig. 1a and Fig. 1b, the integral mesh grid of the flow field of wind turbine blade airfoil in both cases of turbulent and laminar.

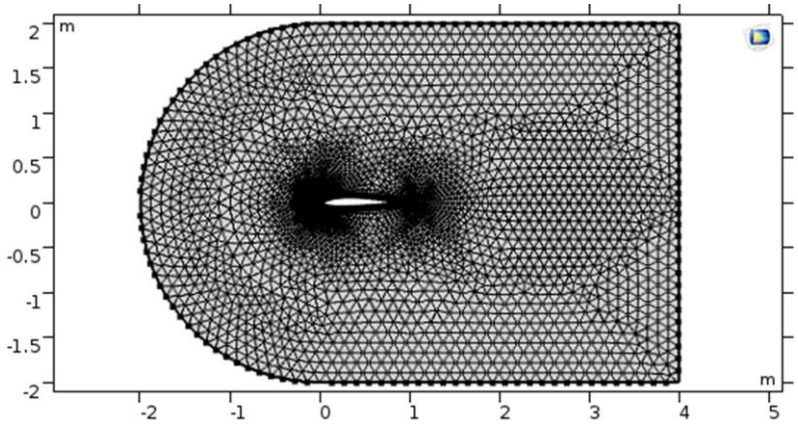

Figure 1a Mesh 1 for optimization model in turbulent air flow

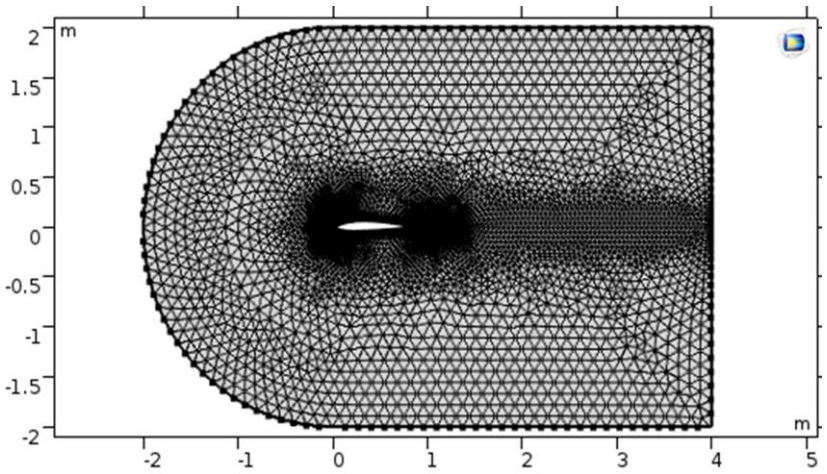

Figure 1b Mesh 2 for optimization model laminar air flow

Table 3. The integral mesh grid

Meshes	**Size 1**	**Size2**
Mesh1 Turbulence Optimization	Domain Elements Fine 7566 elements $0.004 < size < 0.14$	Boundary Elements Finer 204 elements $0.0016 < size < 0.112$
Mesh2 Laminar Optimization	Domain Elements Fine 12072 elements $0.004 < size < 0.14$	Boundary Elements Extra Fine 234 elements $0.0004 < size < 0.052$

3. Results and Discussion

This study was conducted using COMSOL 5.3 simulation software for NACA airfoil PMXX series. Airfoil used in this study has asymmetrical structure and the airfoil is varying in thickness and operating Reynolds number. The lift and drag coefficient were calculated using the same method and graphs were generated for lift and drag coefficient, lift to drag ratio, pressure and velocity distributions over airfoil surface. At the beginning, numerical analysis of the initial airfoil NACA 2414 was performed, and then the optimized airfoil has been compared with the original NACA2414 airfoil. The comparison figures and tables are given in the next sections.

3.1 Influence of Angle of Attack Optimization on Aerodynamic and Shape Of Airfoil

Lift to drag ratio of NACA were calculated, analyzed and presented in Figure 2a. According to Figure 2a, lift to drag ratio increase with the increasing operating Reynolds number. Lift coefficient increment is proportional to the Reynolds number at the same time and during optimization process the highest angle of attack is associated with low Reynolds number but it is not after 10 degree. The performance becomes maximum at optimized angle of attack varying from 4.65 to 5.85 degree with increasing Reynolds number as shown in Fig 2b.

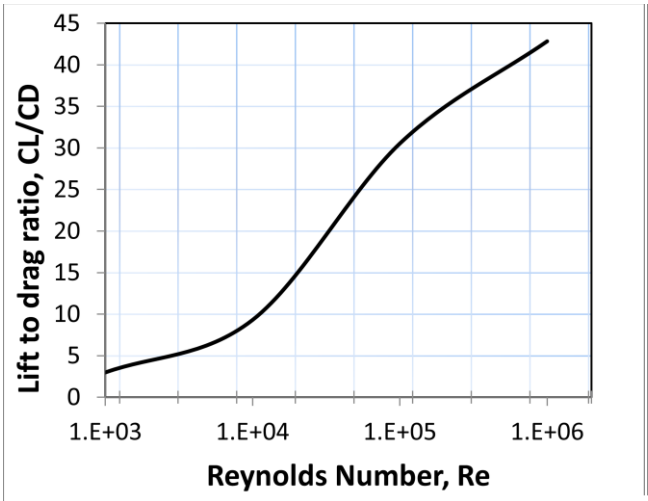

Figure 2a. The effect variation of Reynolds number on CL/CD

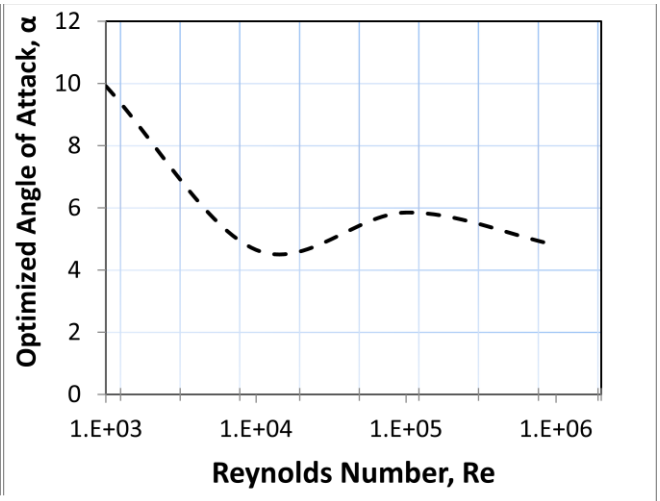

Figure 2b. The effect variation of Reynolds number on angle of attack

After optimization, airfoils in table (4) had lift coefficients 9.5, 5, 3.37 and 2.8 times greater than initial airfoil, the airfoils had drag coefficients 1.3,1.38, 1.5 and 1.4 times greater than initial

airfoil, and the airfoil had lift to drag ratio 7.2, 3.7, 2.2 and 2.0 times greater than initial airfoil, the optimal angle of attack changes from $\alpha = 9.91^{o}$, 4.65^{o},5.85^{o} and 4.8^{o} for Re $=10^{3}$,10^{4},10^{5},and 10^{6} respectively. It can be seen that all airfoils with different Reynolds number requires a positive angle of attack. However, with increasing Reynolds, the increase in the optimized lift coefficient and lift to drag ratio becomes slow when it is compared to initial airfoils, and the drag coefficient increase at the same time, and the maximum of drag coefficients are increased in low rate with Re $= 10^{3}$ to 10^{5}.

Table 4. Aerodynamic Characteristics and Optimized Angle of Attack in Different operating Re Number before and After optimization

Cases	Re	CL	CD	CL/CD	α^{O}
$(NACA2414)_{initial}$	10^{3}	0.05392	0.1308	0.4121	0^{O}
$(NACA2414)_{optimal}$	10^{3}	0.5122	0.1716	2.989	9.91^{O}
$(NACA2414)_{initial}$	10^{4}	0.1098	0.04371	2.513	0^{O}
$(NACA2414)_{optimal}$	10^{4}	0.5553	0.05965	9.310	4.65^{O}
$(NACA2414)_{initial}$	10^{5}	0.2693	0.0198	13.6	0^{O}
$(NACA2414)_{optimal}$	10^{5}	0.9074	0.02971	30.54	5.85^{O}
$(NACA2414)_{initial}$	10^{6}	0.2923	0.0137	21.33	0^{O}
$(NACA2414)_{optimal}$	10^{6}	0.8165	0.01907	42.84	4.80^{O}

The optimization tool needs to be able to change the operating Reynolds number of the airfoil, to obtain an optimum angle of attack (α). The airfoils were optimized directly with the maximum lift to drag ratio as the objective function. Change in the Reynolds number reflect change aerodynamic characteristics. As Reynolds number changes, the angle of attack needs to be adjusted to ensure that the blade operates under optimal conditions. distribution of the geometric shape is kept unchanged, only to reveal the influence of Reynolds number and the associated optimal angle of attack. The aim of this paper is to identify and assess CFD model that can be efficiently coupled with an optimization approach and that is capable to correctly predict the airfoil performance from Re $= 10^{3}$ to 10^{6}, which cover most wind turbines.

(a) After optimization **(b) Before optimization**

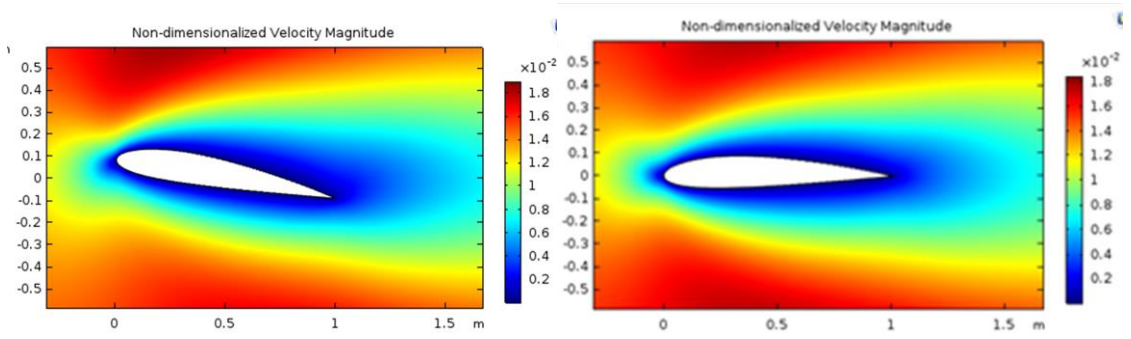

Figure. 3 Velocity distribution at Reynolds number of $\mathbf{10^3}$

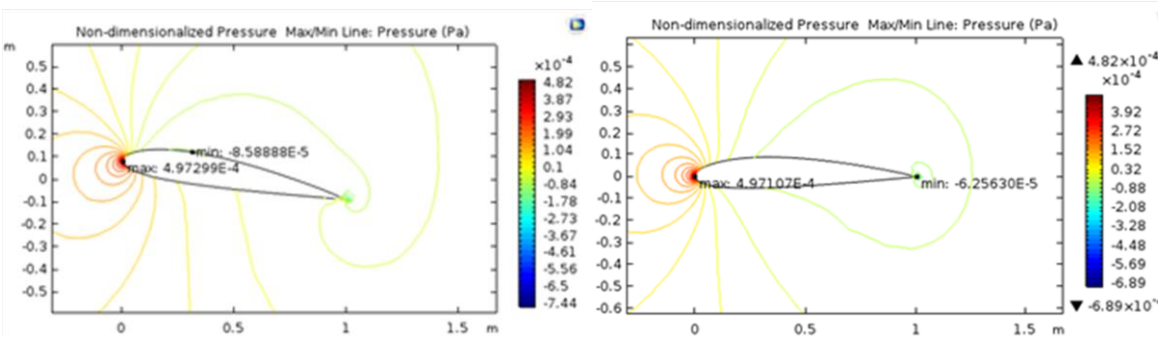

Figure. 4 Pressure distribution at Reynolds number of $\mathbf{10^3}$

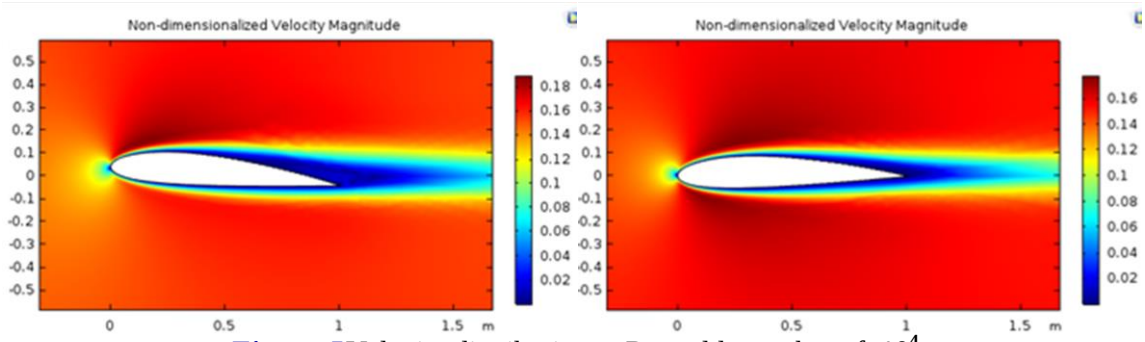

Figure. 5 Velocity distribution at Reynolds number of $\mathbf{10^4}$

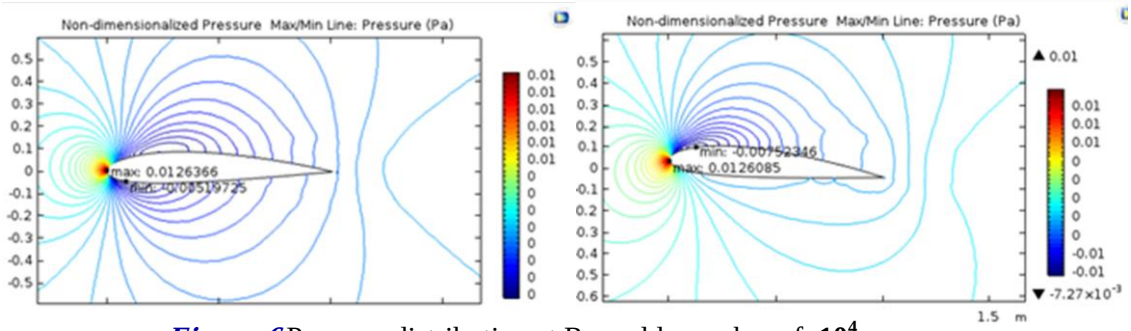

Figure. 6 Pressure distribution at Reynolds number of $\mathbf{10^4}$

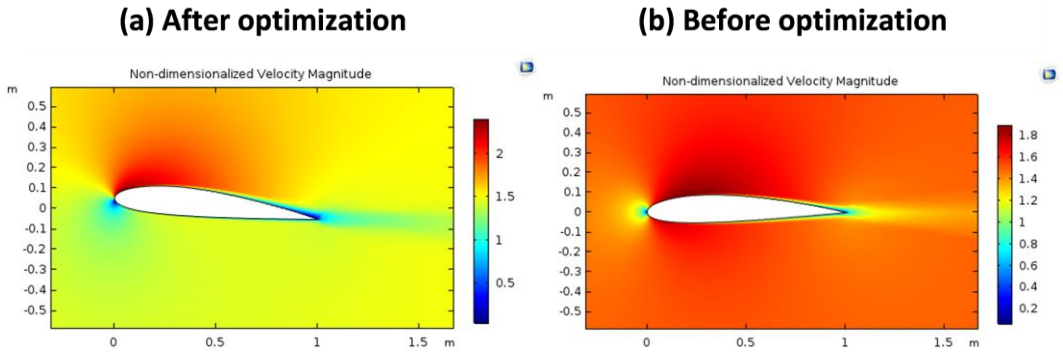

Figure. 7 Velocity distribution at Reynolds number of $\mathbf{10^5}$

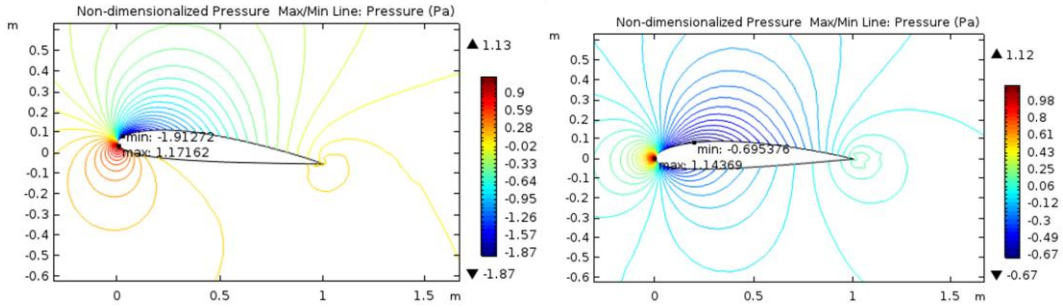

Figure. 8 Pressure distribution at Reynolds number of $\mathbf{10^5}$

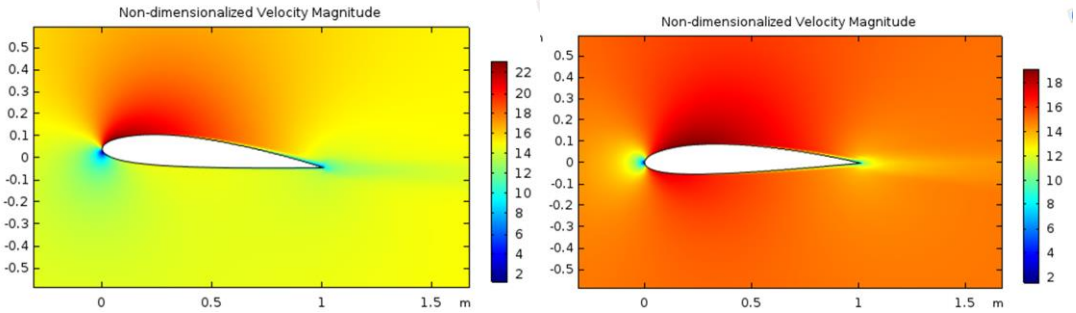

Figure. 9 Velocity distribution at Reynolds number of $\mathbf{10^6}$

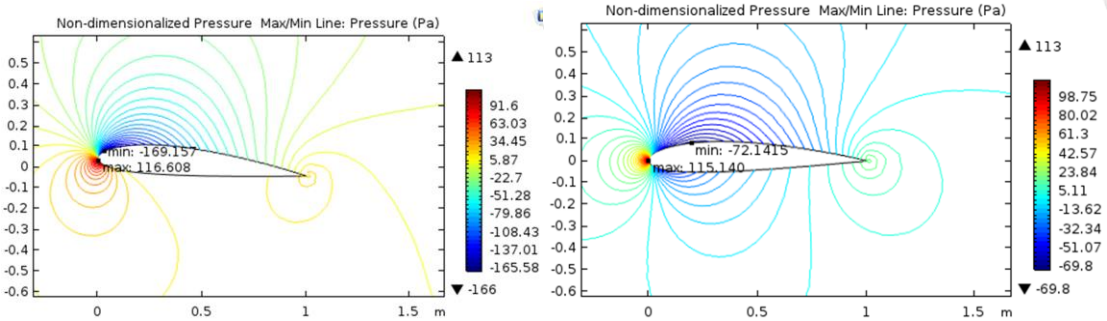

Figure.10 Pressure distribution at Reynolds number of $\mathbf{10^6}$

Figures (3-10) show that the Reynolds number effects the pressure and velocity distribution, with increasing Reynolds number the boundary layers (blue color) become thinner, but more powerful, the velocity was very small and concentrating in point at mid of leading edge before optimization, while the velocity was concentrated in point lower to the mid after optimization. the leading edge experienced high pressure, while the trailing edge experience low pressure, the large Reynolds number , the greater the difference in pressure was between the upper and lower surfaces of airfoil was symmetrical in laminar for Re= 10^3. when the Reynolds number is large, the stall angle of attack of the airfoil were optimized at varying values between 4.65^o and 5.85^o . At wide range of *Reynolds number*, it is evident that the lift increases and drag decreases with *Re* for initial angles of attack (α= 0°) and the geometric parameters

It is obvious that the optimized airfoil has the larger laminar zone than the initial airfoil. In Figure 3-10 the reverse flow zone of the initial airfoil is bigger. So the drag of the optimized airfoil is smaller than the initial airfoil. And the optimized airfoil has the larger velocity than the initial airfoil at the upper airfoil. So the dynamic pressure of the optimized airfoil is bigger and the lift is larger than the initial airfoil and the pressure of the upper airfoil increases near the trailing edge for the optimized airfoil. So the lift of the optimized airfoil is larger than the initial airfoil.

3.2 Influence of Camber Optimization on Aerodynamic and Shape Of Airfoil

The optimization tool also, in compared with the previous case, it needs to be able to change the shape of the airfoil, it must be able to directly to modify its external shape by change maximum thickness of airfoil to obtain an optimum the maximum camber and its position along the chord line. The objective of this study is to optimize an airfoil that is to be used. Since the maximum camber *m* and its position *p* are codependent and both have been optimized at the same time.

The initial and optimized airfoil are shown in figures (13-20). the leading edge airfoil has changed and camber of the airfoil has transformed and increased, after optimization of aerodynamic airfoil shape, local improvement and modification of the blades shape are commonly made based on initial blade shape parameter in order to achieve high maximum performance. As the shape of the airfoil changes, the flow around it also changes, this leads to an alternated pressure distribution which, in turn modifies the aerodynamics properties of the model. Clearly, the pressure distribution are sensitive to changes of geometry. As the camber increases, the tendency to upper surface boundary layer separation become more significant. It can be seen also as the optimal camber increased, the airfoil takes an asymmetry form and is typically used to control its zero -lift angle of attack.

Based on CFD modeling and its optimization method, the airfoil were optimized directly with the maximum lift to drag ratio as the objective. It can be seen from table (5) for all selected relative thickness (*thickness* = 0.08, 0.12, 0.16, 0.2) that aerodynamic performance and the camber before

and after optimization. After optimization, the airfoil had lift coefficient 4 times greater than initial airfoil, the airfoil had drag coefficient 1.5 times greater than initial airfoil, and the airfoil had lift to drag ratio 2.6 times greater than initial airfoil.

On the other side, the maximum camber maximally increases by about 4 times of initial camber and its position is moving further forward by about 0.02-0.12 times from its initial position, when angle of attack ($\alpha=0^{o}$) and Reynolds number ($Re=10^{5}$) were kept constant. The optimal airfoils have a little changes in locations of cambers, but their effect were effective on its thickness. This small amount of change in camber positions allows an increase of the lift coefficients and performance of airfoils.

If the camber is increased, the maximum lift coefficient will be increased, However, with increasing thickness, the increase in the lift coefficient becomes slow, and the drag coefficient increase at the same time, and the increments of drag coefficients are different with different airfoil, when the position of maximum camber is further forward, the maximum lift coefficient becomes large. Hence, the selection of design variables has a significant impact in optimization processes, the thickness of the camber and its position are very important in geometric of the airfoil.

Table 5. Aerodynamic Characteristics and Optimized Camber and its position in Different max. thickness before and After optimization

Case	**th**	**cl**	**cd**	**Cl/cd**	**m**	**p**
$(NACA2408)_{initial}$	0.08	0.225	0.016	13.46	0.02	0.40
$(NACA2408)_{optimal}$	0.08	0.986	0.027	36.01	0.085	0.45
$(NACA2412)_{initial}$	0.12	0.216	0.019	11.11	0.02	0.40
$(NACA2412)_{optimal}$	0.12	0.910	0.031	28.91	0.081	0.46
$(NACA2416)_{initial}$	0.16	0.198	0.023	8.47	0.02	0.40
$(NACA2416)_{optimal}$	0.16	0.798	0.035	22.45	0.078	0.42
$(NACA2420)_{initial}$	0.20	0.168	0.028	5.88	0.02	0.40
$(NACA2420)_{optimal}$	0.20	0.685	0.043	15.68	0.081	0.41

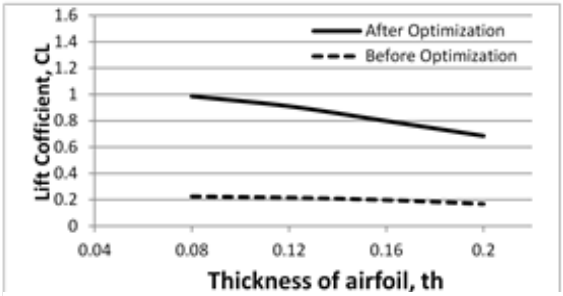

Figure 11a. The effect of variation thickness of airfoil on CD

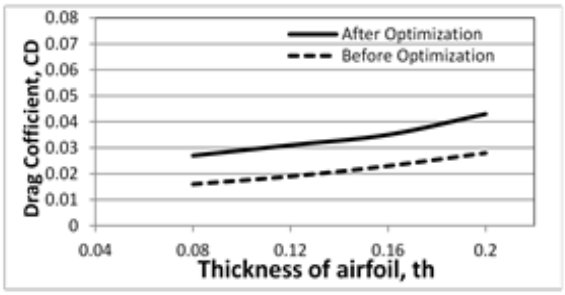

Figure 11b. The effect of variation thickness of airfoil on CL

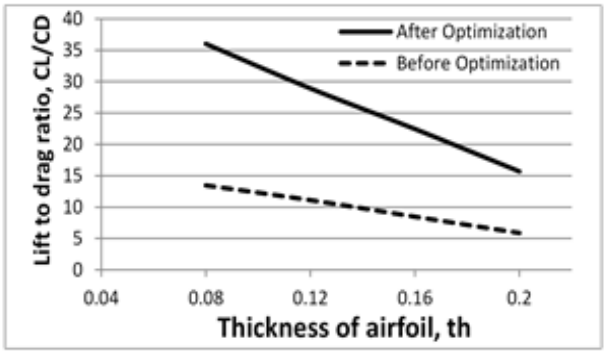

Figure 11c. The effect of variation thickness of airfoil on CL/CD

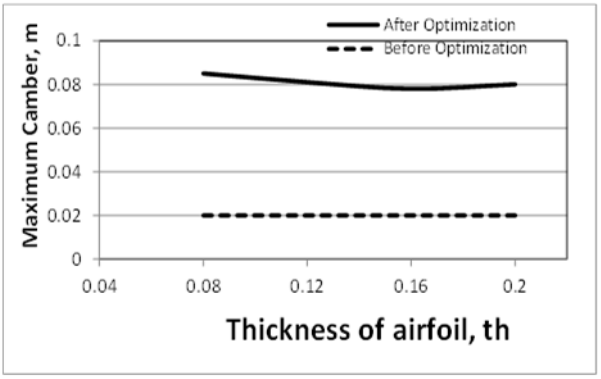

Figure 12. The effect of variation thickness of airfoil on maximum camber

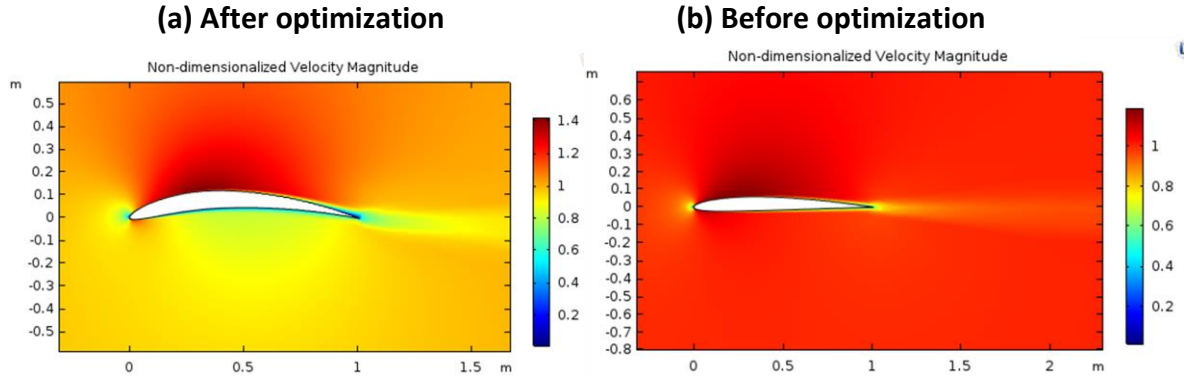

Figure. 13 Velocity distribution at maximum relative thickness of 8% of the chord

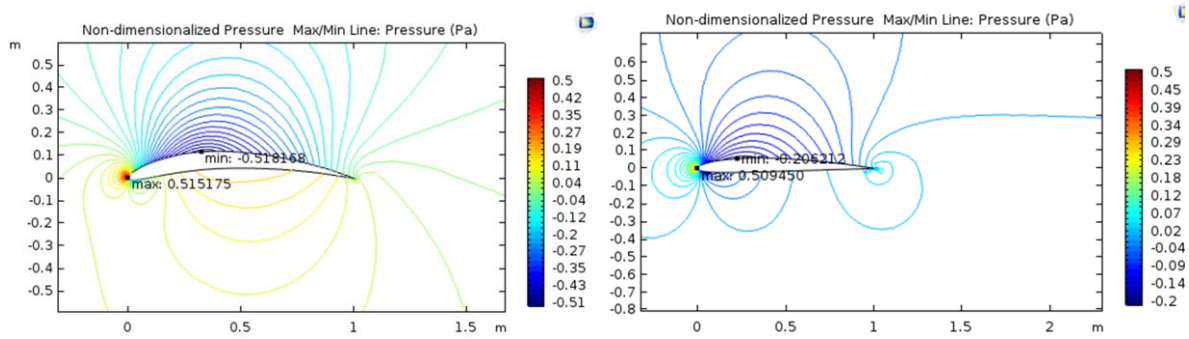

Figure. 14 Pressure distribution at maximum relative thickness of 0. 8% of the chord

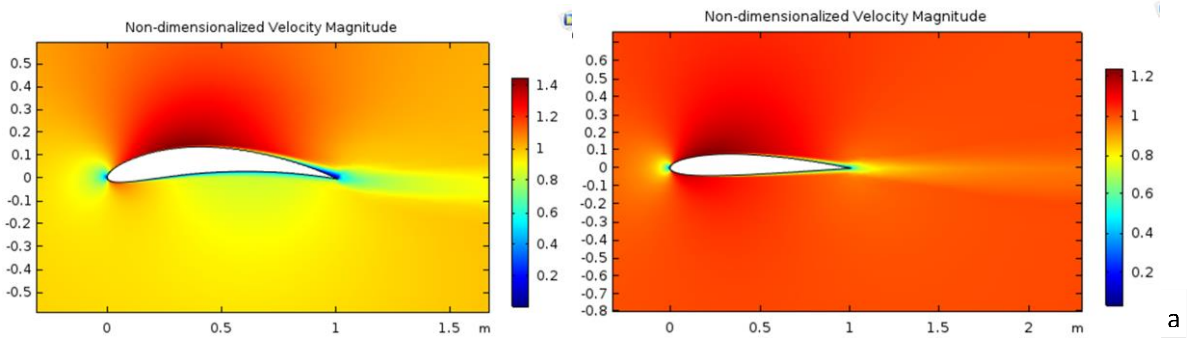

Figure. 15 Velocity distribution at maximum relative thickness of 12% of the chord

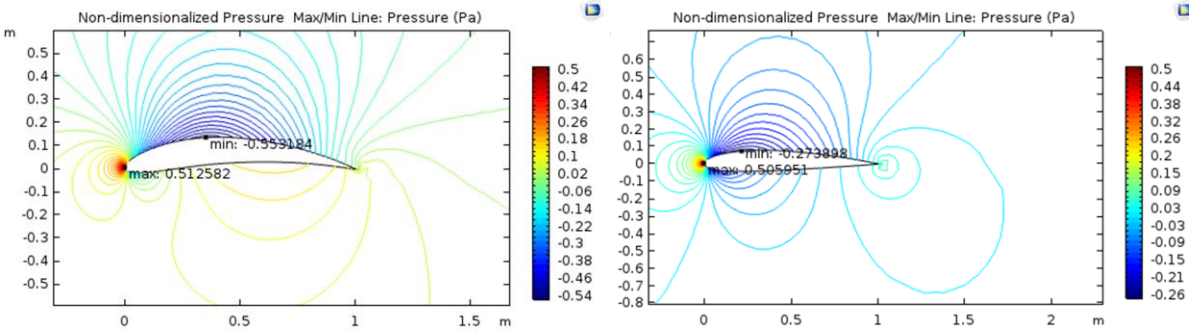

Figure. 16 Pressure distribution at maximum relative thickness of 12%of the chord

(a) after optimization **(b) before optimization**

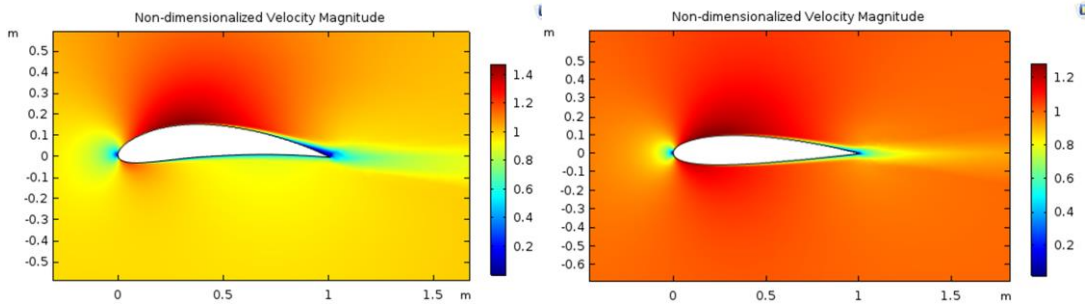

Figure. 17 Velocity distribution at maximum relative thickness of 16% of the chord

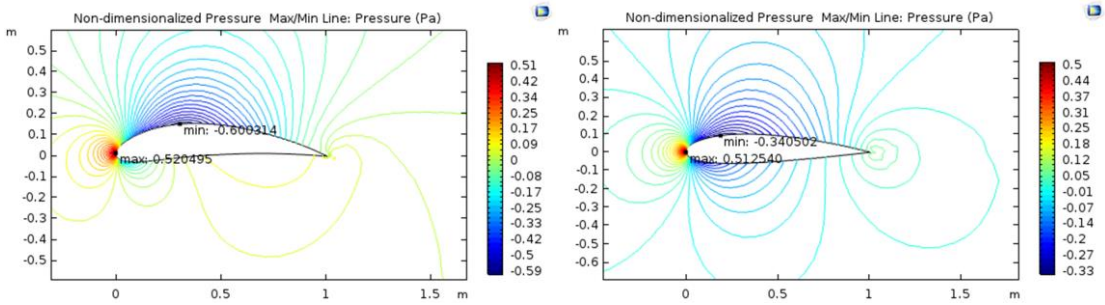

Figure. 18 Pressure distribution at maximum relative thickness of 16% of the chord

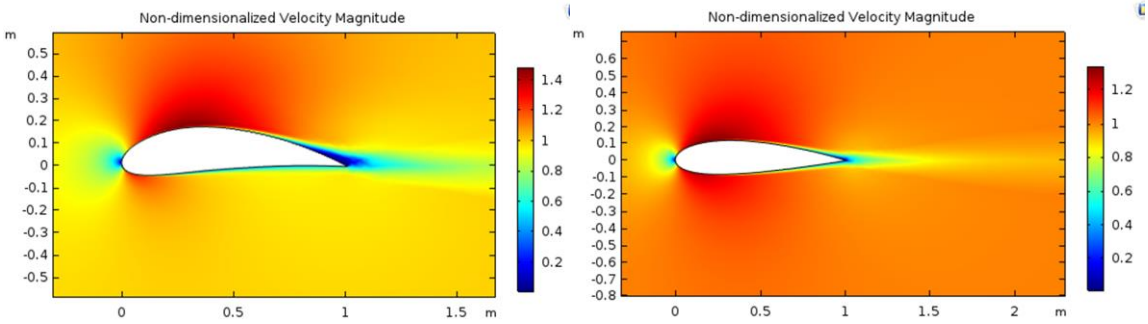

Figure. 19 Velocity distribution at maximum relative thickness of 20% of the chord

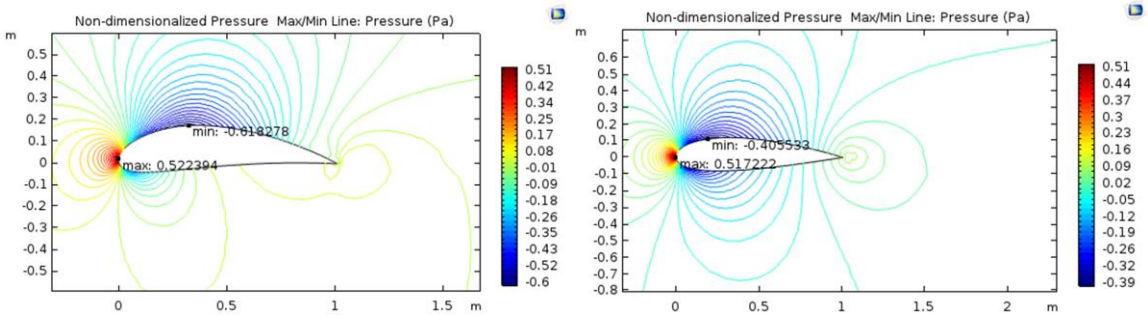

Figure 20 Pressure distribution at maximum relative thickness of 20% of the chord

Conclusions

NACA 2414 wind turbine blade airfoil was selected as the research subject. The effect of Reynolds number on airfoil is studied, and the pressure and velocity distributions on NACA2414 airfoils by varying Reynolds numbers from 10^3 to 10^6 are plotted. The optimal airfoil is used for calculating the higher lift coefficient and lift to drag ratio . The optimum angle of attack corresponding higher lift to drag ratio at constant Reynolds numbers is identified. The effect of angle of attack on coefficient of lift is also predicted for NACA2414 airfoils. At each condition of operating Reynolds number, each airfoils has a particular sitting of the blade airfoil at stalling angle of attack The effect of optimal airfoil camber on the improvement of aerodynamic efficiency has been investigated on four airfoils (NACA 2408, 2412, 2416and 2420). The compromised camber at each four cases has changed from 2% in NACA to (8.5% , 8.1%, 7.8% and 8.1%) of airfoil chord. Therefore, it is more practical to improve the performance, changing the original airfoil NACA before optimization by (NACA 8408, 8412, 8416and 8420) after optimization

References

[1] AAtaei, M Biglari, MNedaei, EAssareh, J KChoi, CYoo, M S Adaramola. Techno-economic feasibility study of autonomous hybrid wind and solar power systems for rural areas in Iran, a case study in Moheydar village. Environmental Progress & Sustainable Energy, 2015, 34(5): 1521–1527

[2] Mahmoodi, E., Jafari, A., Keyhanib, A. (2015) Wind Turbine Rotor Simulation via CFD Based Actuator Disc Technique Compared to Detailed Measurement. Int.Journal of Renewable Energy Development. 4 (3) 205-210.

[3] "Navigant Research." Navigant Research World Market Update 2012 Comments. Web. 08 Nov. 2013.

[4] A. M. Muftah "3D Fluid in an Elbow Meter-CFD Model" SUSJ Journal, Sirte University, Vol. 4, Issue 1, June 2014

[5] A. Muftah "CFD Modeling of Elbow and Orifice Meters" SUSJ Journal, Sirte University, Vol. 7, Issue 1, June 2017, pp 15-32

[6] Tully, S. and Viola, I.M. (2016), "Reducing the wave induced loading of tidal turbine blades through the use of a flexible blade", International Symposium on Transport Phenomena and Dynamics of Rotating Machinery (ISROMAC 2016), 10-15 April, Honolulu, Hawaii, p. 9, available

[7] Hansen, M.O.L., Sørensen, J.N., Voutsinas, S., Sørensen, N. and Madsen, H.A. (2006), "State of the art in wind turbine aerodynamics and aeroelasticity", Progress in Aerospace Sciences, Vol. 42 No. 4, pp. 285-330

[8] Barlas, T.K. and van Kuik, G.A.M. (2010), "Review of state of the art in smart rotor control research for wind turbines", Progress in Aerospace Sciences, Vol. 46, pp 1-27

[9] Lachenal, X.S., Daynes, P.M. and Weaver, (2013), "Review of morphing concepts and materials for wind turbine blade applications", Wind Energy, Vol. 16 No. 2, pp. 283-307

[10] Tully, S. and Viola, I.M. (2016), "Reducing the wave induced loading of tidal turbine blades through the use of a flexible blade", International Symposium on Transport Phenomena and Dynamics of Rotating Machinery (ISROMAC 2016), 10-15 April, Honolulu, Hawaii, p. 9

[11] Stanewsky, E. (2001), "Adaptive wing and flow control technology", Progress in Aerospace Sciences, Vol. 37 No. 7, pp. 583-667

[12] Barbarino, S., Bilgen, O., Ajaj, R.M., Friswell, M.I. and Inman, D.J. (2011), "A review of morphing aircraft", Journal of Intelligent Material Systems and Structures, Vol. 22 No. 9, pp. 823-877

[13] Kuder, I.K., Arrieta, A.F., Raither, W.E. and Ermanni, P. (2013), "Variable stiffness material and structural concepts for morphing applications", Progress in Aerospace Sciences, Vol. 63, pp. 33-55

[14] Smith, A.M.O. (1975), "High-lift aerodynamics", Journal of Aircraft, Vol. 12 No. 6, pp. 501-530

[15] Lissaman, P.B.S. (1983), "Low-Reynolds-number airfoils", Annual Review of Fluid Mechanics, Vol. 15, pp. 223-239

[16] Hicks, R.M. and Henne, P.A. (1978), "Wing design by numerical optimization", Journal of Aircraft, Vol. 15 No. 7, pp. 407-412

[17] Srinath, D.N. and Mittal, S. (2010), "Optimal aerodynamic design of airfoils in unsteady viscous flows", Computer Methods in Applied Mechanics and Engineering, Vol. 199, Nos 29/32, pp. 1976-1991

[18] Minervino, M., Vitagliano, P.L. and Quagliarella, D. (2016), "Helicopter stabilizer optimization considering rotor downwash in forward-flight", Aircraft Engineering and Aerospace Technology, Vol. 88 No. 6, pp. 846-865

[19] Kulfan, B.M., 2007. A universal parametric geometry representation method-"CST". 45th AIAA Aerospace Meeting & Exhibit, Reno, Nevada, USA.

[20] Bu YP, Song WP, Han ZH. 2013. Aerodynamic optimization design of airfoil based on CST parameterization method. J. Northw. Polytech. Univ. 31, 829–835

[21] peigin, S.E., Epstein, B.: Robust Optimization of 2D Airfoils Driven by Full Navier-Stokes Computations. Computers &Fluids. 33, 1175-1200 (2004)

[22] Sobieczky, H.: Parametric Airfoils and Wings. In. Fuji. K., Dulikravich, G.5.(EDS) Notes on Numerical Fluid Mechanics. Vol 68. Wiesbaden, Viewing (1998)

[23] Derksen, R. W., Rogalsky, T.: Bezier-PARSEC. An optimized Airfoil parameterization for Design. Advances in Engineering Software, 41, 923-930 (2010)

[24] Abbott, I.H., Von Doenhoff A.E. Theory of Wing Sections. Dover publications. Newyork (1959)

[25] Hand M. M., Simms D. A. Unsteady aerodynamics experiment phase VI: wind tunnel test configurations and available data campaigns. National Renewable Energy Laboratory, Technical reportr, NREL/ TP 2500-29955, 2001.

[26] Schepers J. G., Feigl L., Rooij R. V., Bruining A**.** Analysis of detailed aerodynamic field measurements using results from an aeroelastic code. Wind Energy, Vol. 7, Issue 4, 2004, p. 357-372

[27] Lindenburg C. Investigation into rotor blade aerodynamics. Report Number ECN-C-03-025, 2003.

[28] A. Muftah " CFD Modeling of Airfoil of wind turbine under different effect of operating conditions" SUSJ Journal, Sirte University, Vol. 9, Issue 1, June 2019, pp 27-43.